http://dx.doi.org/10.5012/bkcs.2011.32.9.3395

Spectroscopic and Morphological Investigation of Copper Oxide Thin Films Prepared by Magnetron Sputtering at Various Oxygen Ratios

Juyun Park, Kyounga Lim,[†] Rex D. Ramsier,[†,‡,§] and Yong-Cheol Kang[*]

Department of Chemistry, Pukyong National University, Busan 608-737, Korea. [*]E-mail: yckang@pknu.ac.kr
Departments of [†]Physics, [‡]Chemistry and [§]Office of Academic Affairs, The University of Akron, Akron, OH, 44325, USA
Received June 22, 2011, Accepted July 29, 2011

Copper oxide thin films were synthesized by reactive radio frequency magnetron sputtering at different oxygen gas ratios. The chemical and physical properties of the thin films were investigated by X-ray photoelectron spectroscopy (XPS), scanning electron microscopy (SEM), atomic force microscopy (AFM), and X-ray diffraction (XRD). XPS results revealed that the dominant oxidation states of Cu were Cu^0 and Cu^+ at 0% oxygen ratio. When the oxygen ratios increased above 5%, Cu was oxidized as CuO as detected by X-ray induced Auger electron spectroscopy and the $Cu(OH)_2$ phase was confirmed independent of the oxygen ratio. The valence band maxima were 1.19 ± 0.09 eV and an increase in the density of states was confirmed after formation of CuO. The thickness and roughness of copper oxide thin films decreased with increasing oxygen ratio. The crystallinity of the copper oxide films changed from cubic Cu through cubic Cu_2O to monoclinic CuO with mean crystallite sizes of 8.8 nm (Cu) and 16.9 nm (CuO) at the 10% oxygen ratio level.

Key Words : Copper oxide, XPS, RF magnetron sputtering

Introduction

Copper films have attracted attention for replacing Al-based interconnects and for ultra-large scale integration devices due to their low electrical resistance, high stability against void formation, and excellent electromigration properties.[1-4] The reliability of Cu interconnects is an important factor that determines the longevity of microelectronic devices, which is complicated by the fact that the native oxide layer on Cu surfaces is not self-protective and Cu oxidizes continuously in air even at room temperature.[5] Therefore it is very important to understand the oxidation behavior of Cu films. Here we focus on spectroscopic and morphological analysis of Cu and Cu-oxide films to better understand surface oxidation phenomena.

Several methods have been used to prepare Cu oxide thin films, including thermal oxidation,[6] chemical conversion,[7] chemical brightening,[8] spraying,[9] plasma evaporation,[10] and reactive sputtering.[11] Many investigations have used magnetron sputtering for preparation of Cu films[12,13] as well. In this research, reactive radio frequency (RF) magnetron sputtering was used to prepare Cu and Cu oxide films with various oxygen ratios in the sputtering gas. For better understanding of surface oxidation, the chemical and physical properties of the deposited thin films were examined by X-ray photoelectron spectroscopy (XPS), scanning electron microscopy (SEM), X-ray diffraction (XRD), and atomic force microscopy (AFM).

Experimental Section

The thin films were prepared on p-type Si(100) wafers at room temperature using reactive radio frequency (RF, 13.56 MHz) magnetron sputtering. Various oxygen ratios in the sputtering gas were used to examine the effect on the surface oxidation of Cu. The Si substrate was mounted on the sample holder above the Cu metal target after following a known cleaning process to remove the native oxide layer.[14] The base pressure of the deposition chamber was kept at 5.0×10^{-7} Torr, and the working pressure was maintained at 48 ± 1 mTorr. During RF sputtering the total gas flow rate was kept at 20 sccm with varying $Ar:O_2$ ratios.

The chemical nature of the films was examined by XPS (VG MultiLab 2000, UK). The energy analyzer of the XPS system is a concentric hemispherical analyzer (CHA). The base pressure in the analysis chamber was maintained lower than 1×10^{-10} Torr and a monochromatic Al Kα (1486.6 eV) X-ray source was used (225 W; filament current 4.2 A). The parameters for survey scans were: pass energy 50 eV; dwell time 50 ms; and energy step 0.5 eV in constant analyzer energy (CAE) mode. High resolution XP spectra were obtained at a pass energy of 20 eV, an energy step of 0.05 eV, and other parameters the same as for survey scans. High resolution XPS data were deconvoluted using XPSPEAK software (version 4.1).

The morphology and surface roughness was checked with SEM (HITACHI, S-2400, Japan) and AFM (Veeco Multimode Digital Instruments Nanoscope III system, USA). The roughness of the films was measured as root mean square (rms) values. XRD (PHILIPS, X'Pert-MPD System, Netherlands) experiments were performed for phase identification with the diffraction patterns collected with Cu Kα (0.154056 nm) radiation in glancing mode with a step size of 0.02 degree.

Results and Discussion

Spectroscopic Analysis. The chemical states of the films were examined with XPS. Figure 1(a) shows high resolution Cu 2p doublet XP spectra from films obtained at different O_2 ratios. The samples are denoted such that, for example, Cu-O_2-60 represents films obtained using 60% O_2 in the sputtering gas. Charging effects in all the XP spectra were corrected with reference to adventitious C 1s at 284.6 eV.[15] When the O_2 ratio was 0%, sharp Cu $2p_{3/2}$ and $2p_{1/2}$ doublet peaks were observed at 932.8 and 952.6 eV, respectively, with spin-orbit splitting (SOS) of 19.8 eV, small shoulder peaks near 935 and 955 eV, and satellite peaks 9 eV above the main features.[16] The main sharp Cu 2p peak indicates that the formation of metallic Cu (Cu^0) and/or monovalent Cu (Cu^+) on the Si wafer is dominant.

The Cu 2p binding energies of Cu^0 and Cu^+ are almost indistinguishable by XPS because the binding energies are superimposed,[16-18] so X-ray induced Auger electron spectroscopy (XAES) was employed in the Cu LMM region to get more information of the oxidation state of Cu (Figure 2). Unlike XP spectra of Cu $2p_{3/2}$, where the oxidation states of Cu^0 and Cu^+ were not resolved, Cu^0 and Cu^+ LMM Auger peaks were resolved[19-21] as shown in Figure 2. The Cu LMM peaks at 918.0, 917.5, and 916.5 eV were assigned to metallic Cu, Cu^{2+}, and Cu^+, respectively. The assigned kinetic energies are consistent with the values reported by Wang *et al.*.[20] In the Cu-O_2-0 films, copper predominantly existed as Cu^0 and Cu^+. After the O_2 ratio increased, the peaks for Cu^0 and Cu^+ diminished and a Cu^{2+} peak evolved. This result indicates that the oxidation state of Cu was heterogeneous with mixing of Cu^0 and Cu^+ in Cu-O_2-0 films which was not distinguishable by XPS. Whereas the satellite peaks detected near 938-947 eV are characteristic of divalent Cu,[17-19] the dominant state of Cu is metallic Cu mixing with a little CuO in our Cu-O_2-0 films as determined by XEAS.

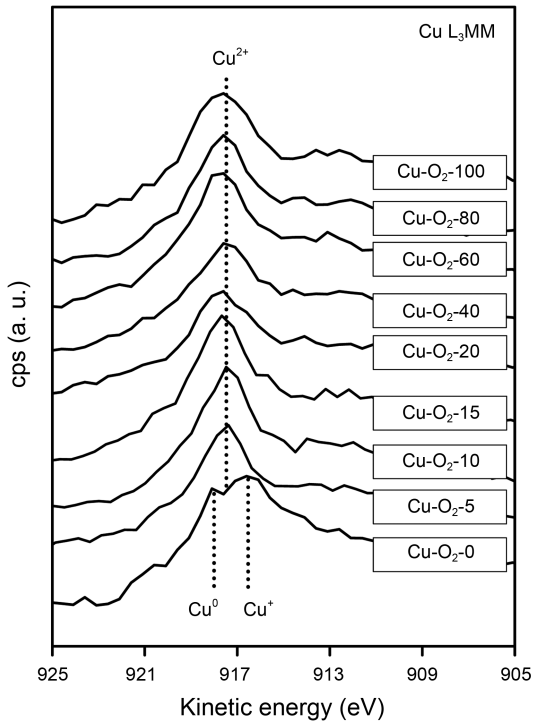

Figure 2. X-ray induced Auger electron spectra (XAES) of Cu LMM region.

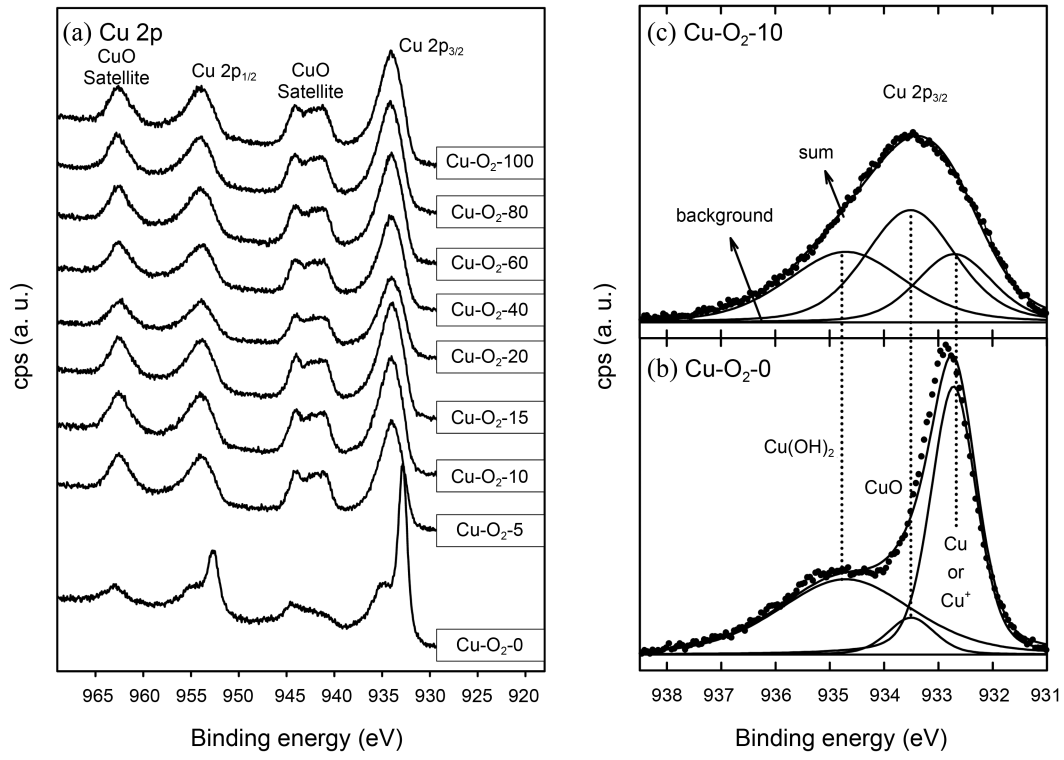

Figure 1. XP spectra of Cu $2p_{3/2}$ region in (a) and representative deconvoluted XP spectra for Cu-O_2-0 in (b) and Cu-O_2-10 in (c).

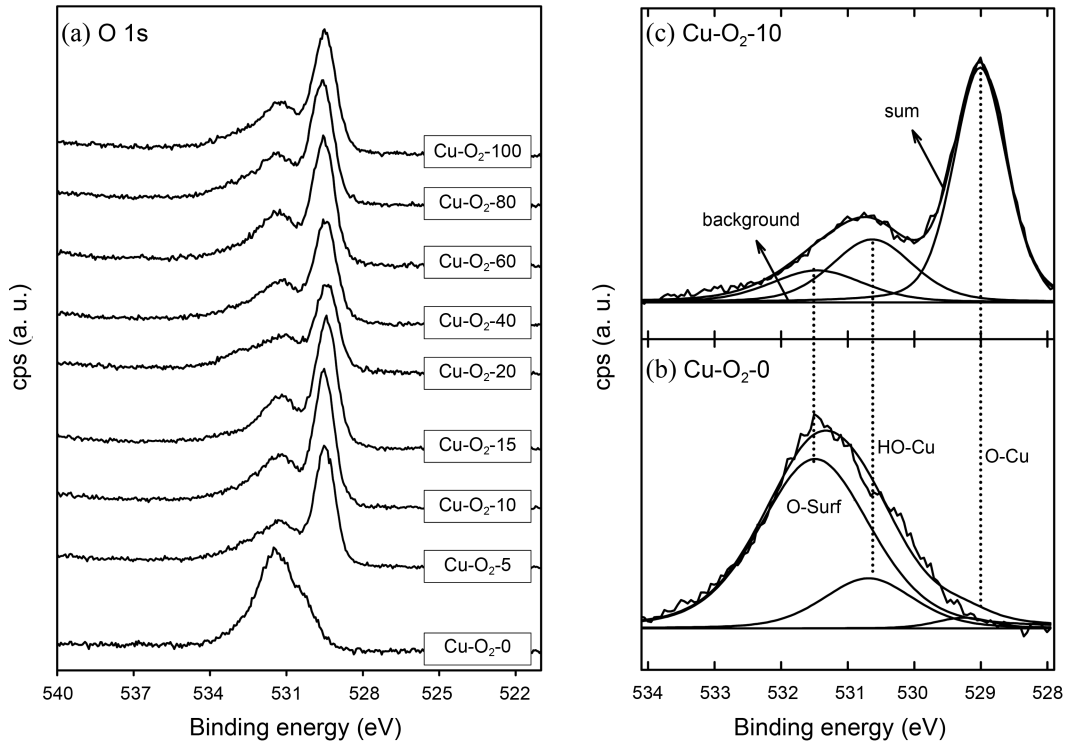

Figure 3. XP spectra of O 1s region (a) and representative deconvoluted XP spectra of Cu-O_2-0 in (b) and Cu-O_2-10 in (c).

When the oxygen ratio increased to 5%, the main Cu $2p_{3/2}$ feature shifted to 934.0 from 932.8 eV and no apparent change was detected with further increases of oxygen. This would indicate that the oxidation of Cu, at the surface of the films, was fully established at the lowest level of O_2 content in the sputtering gas used in this study. In order to get more detailed information of the oxidation state of Cu, the Cu $2p_{3/2}$ binding energy regions were deconvoluted as shown in Figures 1(b) and (c), respectively. Three components were assigned as metallic Cu (Cu^0/Cu^+), CuO, and $Cu(OH)_2$ at 932.7, 933.5, and 934.7 eV, respectively.[6,7] Metallic Cu (and/or Cu^+) was dominant in Cu-O_2-0 film. As the O_2 ratio increased, the oxidation state of Cu changed from metallic to divalent. The content of Cu as CuO in the surface regions of the films increased from 7 to 43% when oxygen was added, whereas the portion of copper associated with $Cu(OH)_2$ was almost constant at 40% for all samples.

Figure 3 shows high resolution XP spectra of the O 1s binding energy region. These data are consistent with those of Figure 1 and verify that Cu was oxidized by the 5% O_2 content. The representative O 1s XP spectra of Cu-O_2-0 and Cu-O_2-10 were deconvoluted as shown in Figures 3(b) and (c), respectively. There were three oxygen components namely O-Cu, HO-Cu, and oxygen on the surface (O-surf) at 529.1, 530.6, and 531.5 eV, respectively. Metallic Cu could attract more oxygen to the surface of the films, leading to the larger concentration of surface oxygen on Cu-O_2-0 than on Cu-O_2-10 films.

We also investigated the valence band region of these films with XPS. In Cu-O_2-0, only Cu 3d was detectable in this region centered at 3 eV below the Fermi level, as shown in Figure 4. The asymmetric factor of Cu 3d in Cu-O_2-0 is smaller than others. This phenomenon might be caused because of the incorporation of O 2p as oxygen ratio increased. As the oxygen ratio increased, the O 2p peak at ca 5 eV evolved by hybridization with Cu 3d. These values are

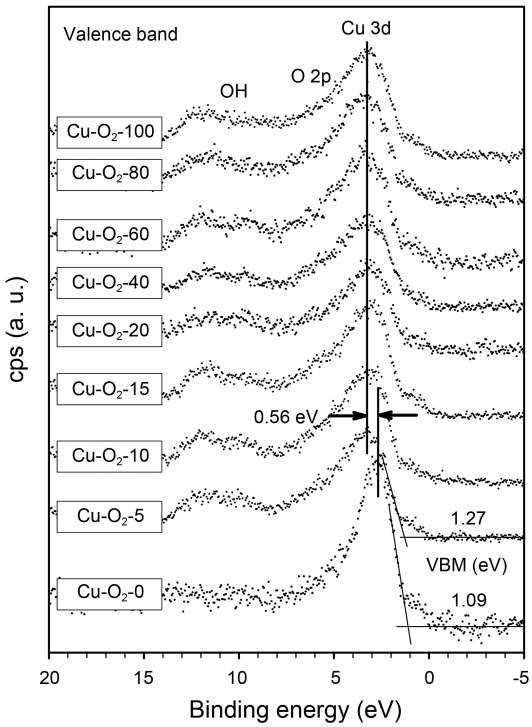

Figure 4. Valence band maximum of copper oxide thin films. The numbers at the right in the figure show VBM values.

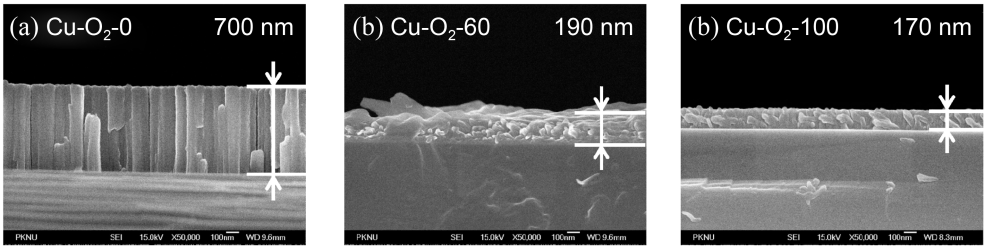

Figure 5. Cross sectional SEM images of Cu oxide thin films on Si(100) at various sputter gas ratios.

consistent with the results from Galakhov *et al*.,[22] who studied the valence bands of Fe 3d, Cu 3d and O 2p theoretically using local spin density approximations (LSDA). Learmonth *et al*. reported a similar result with experimental values of O 2p partial density of states observed at ~2.7, ~4.5, and ~6 eV below the Fermi level [23]. The increase of the partial density of state at 5 eV indicates Cu was oxidized.[24] A hydroxyl peak increases in the 8-13 eV region with increasing oxygen ratio as well.[25]

The valence band maximum (VBM) of each film was determined by extrapolation of the linear portion of valence band edge to the background and the equation for the linear portion was obtained by the least squares method. The representative VBM values before and after introducing oxygen into the sputtering gas are shown in the Figure 4. The VBM values lay in the range 1.19 ± 0.09 eV with different oxygen ratios. Oxygen incorporation during Cu deposition did not shift the VBM but the density of states increased presumably through hybridization of Cu 3d and O 2p states after the formation of CuO. The Cu 3d valence band shifted to higher binding energy (*ca*. 0.56 eV) due to this hybridization.

Morphological Investigation. Representative sectional views of SEM images of Cu oxide thin films obtained by RF sputtering are shown in Figure 5. The film thickness depicted in the figure was determined using the Motic Images Plus 2.0 ML program. The Cu-O_2-0 film grew columnar in shape with column diameters ca 88 nm and film thickness ca 700 nm. As the ratio of O_2 increased during sputtering, the film thickness decreased to about 170 nm. The amount of Ar controls the sputter yield and that of oxygen varies the reactivity on the surface. The sputtering yield was decreased and reactivity was increased, as the percentage of the O_2 in the sputter gas was increased. Therefore, the films grown with higher oxygen concentrations differ from Cu-O_2-0 in that they are thinner and have a different crystal growth morphology shown in Figure 5.

The crystallinity of the films was verified with XRD shown in Figure 6. The phase changed from metallic simple cubic Cu(111) through simple cubic Cu_2O to monoclinic CuO(111) and (002)[26,27] with increasing O_2 ratio in the sputtering gas. The metallic Cu was gradually oxidized to CuO in an oxygenated environment. The crystallite sizes of c-Cu(111) in Cu-O_2-0 and m-CuO(002) in Cu-O_2-10 were determined using Scherrer's equation,[28] $D = (K\lambda)/(B\cos\theta)$, where D, K, λ, θ, and B are the mean crystallite size, the

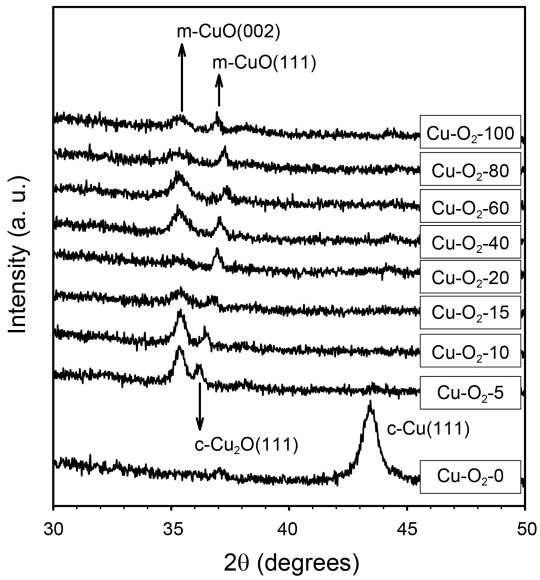

Figure 6. X-ray diffraction patterns of Cu oxide films deposited at various oxygen ratio.

Scherrer's constant (0.9), the X-ray wavelength, Bragg diffraction angle, and full width at half maxima (FWHM) of the diffraction peaks, respectively. The mean crystallite sizes of the c-Cu(111) in Cu-O_2-0 and m-CuO(002) in Cu-O_2-10 were found to be 8.8 and 16.9 nm, respectively.

Finally, the morphology and roughness of the films were analyzed with AFM. Representative 3-D AFM images are shown in Figure 7. When the oxygen ratio increased, the roughness of the copper oxide thin film decreased.[29] The roughness of Cu-O_2-0 was 5.29 nm which reduced to 2.43 ± 0.39 nm by oxide formation. The RMS roughness of the films is shown in Figure 8. The Cu-O_2-0 surfaces were rough as the films grew in columnar shape (Figure 5). Oxygen introduction during RF deposition led to relatively smooth surfaces. The low crystallinity of the oxidized films evidenced by the weak diffraction features of Figure 6 indicate predominantly amorphous growth mechanism resulting in smoother surfaces.

The findings described in this study point to the possibility of tailoring chemically and physically different copper oxide thin films by controlling oxygen ratios during sputtering. Most importantly, these results indicate that further investigations of films produced in very dilute oxygen environments are needed for obtaining fine control over the formation of cuprous (Cu^+) and cupric (Cu^{2+}) oxide thin films. It is this

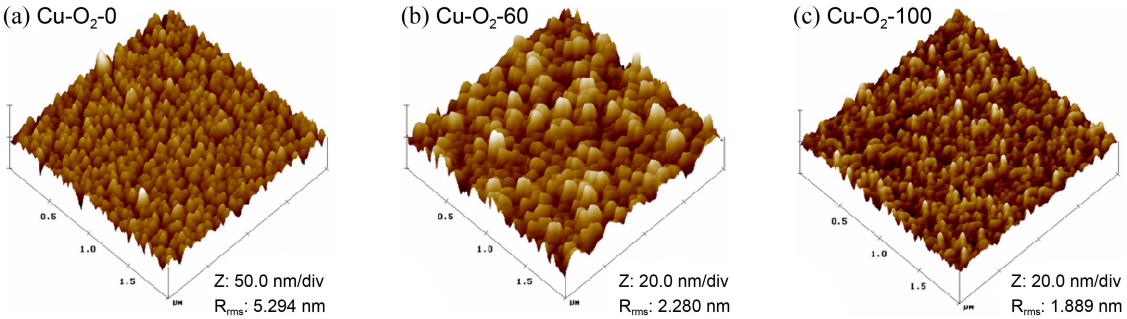

Figure 7. Representative 3-D AFM images of copper oxide thin films. Note the z-scale of the figures.

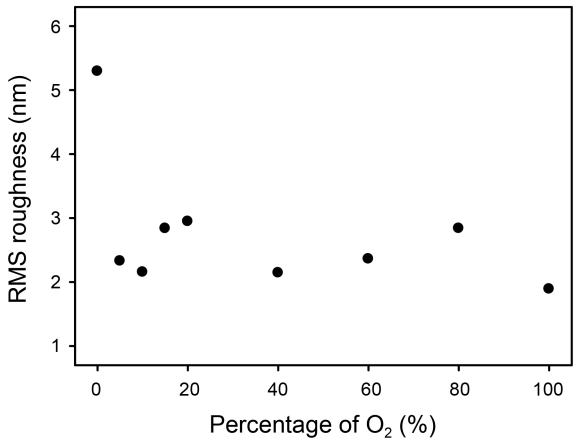

Figure 8. RMS roughness of Cu oxide thin films obtained at various oxygen ratios in the sputtering gas.

fine control that will enable the preparation of thin films with properties optimized for various applications such as photocatalytic hydrogen production and organic and/or inorganic photovoltaic solar cells.

Conclusions

Copper oxide thin films on p-type Si(100) were successfully prepared by reactive RF magnetron sputtering. Chemical investigation of the resulting films was performed by XPS and the oxidation states of Cu was confirmed by XAES. Analysis revealed metallic Cu and Cu_2O were formed in Cu-O_2-0 and that the other films were mainly in the CuO phase. In Cu 2p XP spectra, $Cu(OH)_2$ was also detected in relative amounts that were insensitive to additional oxygen content in the sputtering gas. The values of valence band maxima were almost constant, but the density of states increased after the oxygen was introduced. The thickness and roughness of the films decreased with increasing oxygen ratios. The phase transformation from cubic Cu and Cu_2O to monoclinic CuO was confirmed by XRD and crystallite sizes increased with higher oxygen ratios.

Acknowledgments. This research was supported by Basic Science Research Program through the National Research Foundation of Korea (NRF) funded by the Ministry of Education, Science and Technology (2010-0021332).

References

1. Qu, X. P.; Tan, J. J.; Zhou, M.; Chen, T.; Xie, Q.; Ru, G. P. *Appl. Phys. Lett.* **2006**, *88*, 151912.
2. Yan, M. Y.; Suh, J. O.; Ren, F.; Tu, K. N.; Vairagar, A. V.; Mhaisalkar, S. G. *Appl. Phys. Lett.* **2005**, *87*, 211103.
3. Park, C. W.; Vook, R. W. *Appl. Phys. Lett.* **1991**, *59*, 175.
4. Murarka, S. P.; Gutmann, R. J.; Kaloeros, A. E.; Lanford, W. A. *Thin Solid Films* **1993**, *236*, 257.
5. Suzuki, S.; Ishikawa, Y.; Isshiki, M.; Waseda, Y. *Mater. Trans. JIM* **1997**, *38*, 1004.
6. Gong, Y. S.; Lee, C.; Yang, C. K. *J. Appl. Phys*. **1995**, *77*, 5422.
7. Laurie, A. B.; Norton, M. L. *Mater. Res. Bull.* **1989**, *24*, 213.
8. Laurie, A. B.; Norton, M. L. *Mater. Res. Bull.* **1989**, *24*, 1521.
9. Ottosson, M.; Carlsson, J. O. *Surf. Coat. Technol.* **1996**, *78*, 263.
10. Santra, K.; Sarkar, C. K.; Mukheriee, M. K.; Ghosh, B. *Thin Solid Films* **1992**, *213*, 226.
11. Drobny, V. F.; Palfrey, D. L. *Thin Solid Films* **1979**, *61*, 89.
12. Prater, W. L.; Allen, E. L.; Lee, W. Y.; Toney, M. F.; Kellock, A.; Daniels, J. S. *J. Appl. Phys*. **2005**, *97*, 093301.
13. Pletea, M.; Bruckner, W.; Wendrock, H.; Kaltofen, R. *J. Appl. Phys.* **2005**, *97*, 054908.
14. Ma, C. Y.; Lapostolle, F.; Briois, P.; Zhang, Q. Y. *Appl. Surf. Sci.* **2007**, *53*, 8718.
15. Borg, H. J.; van den Oetelaar, C. C. A.; van Ijzendoorn, L. J.; Niemantsverdriet, J. W. *J. Vac. Sci. Technol. A* **1992**, *10*, 2737.
16. Morales, J.; Caballero, A.; Holgado, J. P.; Espinós, J. P.; González-Elipe, A. R. *J. Phys. Chem. B* **2002**, *106*, 10185.
17. Ai, Z.; Zhang, L.; Lee, S.; Ho, W. *J. Phys. Chem. C* **2009**, *113*, 20896.
18. Yoon, K. H.; Choi, W. J.; Kang, D. H. *Thin Solid Films* **2000**, *372*, 250.
19. Lee, S. Y.; Nguyen, M. N.; Sun, Y. M.; White, J. M. *Appl. Surf. Sci.* **2003**, *206*, 102.
20. Long, J.; Dong, J.; Wang, X.; Ding, Z.; Zhang, Z.; Wu, L.; Li, Z.; Fu, X. *J. Colloid Interface Sci.* **2009**, *333*, 791.
21. Zhang, G.; Long, J.; Wang, X.; Dai, W.; Li, Z.; Wu, L.; Fu, X. *New J. Chem.* **2009**, *33*, 2044.
22. Galakhov, V. R.; Peteryaev, A. I.; Kurmaev, E. Z.; Anisimov, V. I. *Phys. Rev. B* **1007**, *56*, 4584.
23. Learmonth, T.; McGuinness, C.; Glans, P. A.; Kennedy, B.; John, J. S.; Guo, J. H.; Greenblatt, M.; Smith, K. E. *Phys. Rev. B* **2009**, *79*, 8.
24. Scanlon, D. O.; Watson, G. W.; Payne, D. J.; Atkinson, G. R.; Egdell, R. G.; Law, D. S. L. *J. Phys. Chem. C* **2010**, *114*, 4636.
25. Bebensee, F.; Voigts, F.; Maus-Friedrichs, W. *Surf. Sci*. **2008**, *602*, 1622.
26. Yu, Q.; Ma, X.; Lan, Z.; Wang, M.; Yu, C. *J. Phys. Chem. C* **2009**, *113*, 6969.
27. Nakano, Y.; Saeki, S.; Morikawa, T. *Appl. Phys. Lett*. **2009**, *94*, 022111.
28. Langford, J. I.; Wilson, A. J. C. *J. Appl. Cryst.* **1978**, *11*, 102.
29. Tsai, D.-C.; Huang, Y.-L.; Lin, S.-R.; Liang, S.-C.; Shieu, F.-S. *Appl. Surf. Sci.* **2010**, *257*, 1361.